Hindawi
Advances in Astronomy
Volume 2023, Article ID 3527106, 13 pages
https://doi.org/10.1155/2023/3527106

Research Article

Measuring Antenna Elevation Mechanism Pointing Errors with Multiencoder Information Sources

Duoxiang Xu,[1,2] **Qian Xu**,[1,3,4] **Na Wang**,[1,3,4] **and Fei Xue**[1,3,4]

[1]*Xinjiang Astronomical Observatory, Chinese Academy of Sciences, Urumqi 830011, China*
[2]*University of Chinese Academy of Sciences, Beijing 100049, China*
[3]*Key Laboratory of Radio Astronomy, Chinese Academy of Sciences, Urumqi 830011, China*
[4]*Xinjiang Key Laboratory of Radio Astrophysics, Urumqi 830011, China*

Correspondence should be addressed to Qian Xu; xuqian@xao.ac.cn

Received 20 January 2023; Revised 29 March 2023; Accepted 3 April 2023; Published 13 April 2023

Academic Editor: Sándor Frey

There are many factors that cause pointing errors in radio telescopes. As one of the motion positioning mechanisms of the radio telescope, the error caused by the elevation mechanism cannot be ignored. The source of error in the elevation mechanism comes mainly from the key transmission components and the support structure. Accurate measurement of the errors caused by them is the key to analyzing their law of change. Aiming at the main error factors in the antenna elevation mechanism, this study builds a scaled-down experimental platform for the elevation mechanism and proposes an error measurement method based on multiencoder information sources. The method compares the error law of change of the antenna elevation mechanism under different driving modes, different centerline deviations of the bearings, and different backlashes and designs error measurement experiments for the abovementioned operating conditions. The results show that the error measurement method based on multiencoder information sources can accurately measure the error of the antenna elevation mechanism under different driving modes. The method can also accurately reflect the law of change in transmission error when the backlash of the elevation mechanism and the centerline deviation of the bearings increase. The final experimental measurement shows that the driving mode of the dual-motor can eliminate about 70% of the mechanism error caused by the backlash. The average value of the error increases by a factor of 1.9 when the backlash increases from 0.1 mm to 1.26 mm. The average value of the error increases by a factor of 5 when the centerline deviation of the bearings increases from 0 to 1.5 mm. This has a good reference value to correct for the pointing error of a radio telescope.

1. Introduction

For large aperture radio telescopes, accurate pointing is a fundamental requirement for the high-precision measurement of astrophysical targets. At present, the pointing accuracies achieved by large aperture radio telescopes in various countries are at the arcsecond level. The 110 m radio telescope at Xinjiang [1] under construction has a design requirement of 5″ (blind pointing) for pointing accuracy, the SHAO 65 m radio telescope [2] has a pointing accuracy better than 3″ (after observing a local calibrator), and the 100 m radio telescope at Effelsberg [3] has a pointing accuracy of 10″ (blind pointing), and the Green Bank Telescope [4, 5] has a pointing accuracy of 9″ (blind pointing). When higher pointing accuracy is required for radio telescopes to achieve their science goals, it also means that more error factors affecting the pointing accuracy need to be considered, including displacement of the secondary reflector, azimuth track flatness, gravity loading, wind loading, and nonuniform temperature fields.

At present, the research on error factors that affect the accuracy of pointing is mainly classified into two categories. One is the widely used software correction method, which incorporates the major error factors that affect the accuracy of pointing into the antenna pointing correction model to complete the error analysis and correction of the antenna.

Kong et al. proposed a model for the pointing calibration error of the radio telescope, considering the azimuth nonlinear error, which improved the pointing accuracy by 43.6% compared to the linear model [6]. Huang et al. proposed a semiparametric regression model to improve the pointing accuracy of the telescope, and the parameters of the kinematic model were estimated by fitting the statistical model to eliminate geometric and nonlinear errors, which significantly improved the pointing accuracy of the telescope after calibration [7]. The other category starts from each subfactor, affecting the pointing error, and only considers the effects of one or two factors on the antenna pointing error. Chen et al. introduced the axial displacement of the secondary reflector of the telescope to the radio pointing model for SHARC II. The results show that the reconstructed radio pointing model can improve the accuracy of estimating the pointing error [8]. Gawronski et al. and Maneri et al. established a simple and intuitive query table for the pointing error caused by the orbital unevenness. The results from Gawronski et al. show that the pointing error in the elevation direction is reduced from 16.2″ to 5″, and the pointing error in the azimuth direction is reduced from 52.2″ to 11.2″ [9, 10]. Buffa et al. and Nikolic et al. analyzed the effect of gravitational deformation of the telescope's main reflecting surface on the pointing error for the SRT and the GBT, comparing the FEA gravitational deformation results with photogrammetry and updating the FEA model [11, 12]. The effect of wind loading on antenna pointing error was investigated by Hashimoto et al., who measured the dynamic characteristics of the Nobeyama 45 m radio telescope using a piezoelectric accelerometer under wind loading and determined the response frequency and vibration mode of the main reflecting surface [13]. Cho et al. calculated the wind loading data from the Gemini South telescope and analyzed that the average pressure pattern on the Gemini mirror is primarily caused by the interaction of the airflow with the telescope structure [14]. Ukita used the Nobeyama 45 m telescope as a research object and analyzed thermal effects on the antenna pointing error and pointed out that the difference in pointing accuracy between night and day was still 2″ after correction [15]. Fan et al., after analyzing the insolation temperature field of the Five-Hundred-Meter Aperture Spherical Telescope (FAST) in China, pointed out that the deformation due to thermal effects reached 2 mm, considering the breeze environment, accounting for 40% of the total accuracy requirement [16].

For the method of using software to analyze and correct antenna pointing error, due to the wide variety of error factors and the coupling problem between the error factors, it will be difficult to design an effective correction model. Regarding the influence of only one or two factors on the accuracy of antenna pointing, few scholars have carried out relevant research specifically on the impact of antenna pointing accuracy caused by error in the elevation mechanism. As one of the two main antenna positioning mechanisms, the impact of the error in the elevation mechanism on the accuracy of the antenna pointing cannot be ignored. In a study of the shaft angle measurement error of the 50 m radio telescope at the MiYun Station of the National Astronomical Observatory of China, Kong et al. showed that there is a very strong correlation between the shaft angle measurement error of the antenna elevation shaft and the insolation temperature gradient, and the correlation coefficient reaches 76%~99% [17]. Zheng et al. pointed out in the analysis of the pointing error of the radio telescope that in terms of the shafting error, there are driving system errors and shaft angle transmission errors [18].

The elevation mechanism of the radio telescope is mainly composed of transmission components and support structures. Among them, the key transmission components include the elevation gear, the driving gear, and the motor. The key support structure includes the elevation shaft and the support bearings located at both ends of the elevation shaft. Similar to the mechanism errors in the field of electromechanical transmission, the errors caused by the backlash error when the elevation gear meshes with the driving gear and the errors caused by the centerline deviation of the bearings at both ends of the elevation shaft are the main sources of errors in the elevation mechanism. Fernandez-Del-Rincon et al. combined the dynamic characteristics of rolling bearings and gears to propose an improved model, which states that the motion of both gears and bearings involves nonlinearity and will provide different resonant frequencies depending on the transmitted load [19]. Liu et al. investigated the dynamic response of the gear pair system and the interaction relationship between the bearing clearance and the backlash, and the results showed that the bearing clearance is adaptive and that gear separation and gear back meshing are suppressed as the transmitted torque increases [20]. Due to the low speed, heavy load, and high-precision operating conditions of the antenna elevation mechanism, the error correction methods in the field of electromechanical transmission are not fully applicable to the antenna elevation mechanism.

There is little existing research on the effect of the elevation mechanism on telescope pointing accuracy. Therefore, aiming at the factors affecting the pointing errors of radio telescopes, this study proposes a method for measuring the error of the elevation mechanism based on multiencoder fusion, builds a scaled-down experimental platform for the elevation mechanism, and describes the measurement principle and measurement process of the elevation mechanism error in detail. Multiencoder information sources allow us to more rigorously measure the errors of the antenna elevation mechanism under different driving modes, and they also accurately measure the transmission errors caused by the backlash of the elevation mechanism and the centerline deviation of the bearings. Therefore, multiencoder readings and analyses will be useful in improving the correction of pointing errors in the elevation mechanism for large radio telescopes.

2. Analyzing Errors and Building an Experiment Platform

According to the actual working conditions and the working principle of the antenna elevation mechanism, the error of the antenna elevation mechanism is analyzed, and the error

measurement principle is briefly described. Based on this principle, a scaled-down experiment platform of the antenna elevation mechanism is built, and data acquisition with multiencoders is performed.

2.1. The Principle of Error Measurement. When the antenna performs the elevation action, there is a rotational error between the actual elevation angle of the elevation gear and its theoretical elevation angle. The error is a comprehensive error, related to both the backlashes between the elevation gear and the driving gear and the centerline deviation of the bearings at both ends of the elevation shaft. If the elevation shaft is driven by a single motor to perform the antenna elevation action, a transmission error will occur due to the presence of backlash. When the elevation shaft is driven by two motors, each performing the elevation action of the antenna, it serves to eliminate the backlash by mechanical means. If the bearings at both ends of the elevation shaft are installed or run for a long time, there will be a transmission error due to the centerline deviation of the bearings. In order to accurately measure the error caused by the backlashes between the elevation gear and the driving gear, as well as the error caused by the centerline deviation of the bearings at both ends of the elevation shaft, in this study, we utilized a multiencoder information source to measure the real-time position of three key parts of the elevation mechanism: the servo motor, the elevation gear, and the elevation shaft. The measurement principle is shown in Figure 1.

In Figure 1, the elevation shaft passes through the elevation gear and its front and rear ends are mounted, respectively, on the position adjusting device and the bracket through bearings. The position adjusting device has three degrees of freedom, which can adjust the rotation angle θ along the Z axis, the displacement z_1 along the Z axis, and the displacement y_1 along the Y axis of the front end of the elevation shaft. The reduction ratio between the elevation gear and the driving gear is 198:38. The elevation angle of the antenna ranges from 5° to 90°, and the rotation angle of the driving gear ranges from 0° to 443°. When the elevation mechanism performs the elevation action, the encoders located at the ends of the left- and right-hand servo motors output the pulse signal B and the pulse signal A, respectively, to the motion controller. The encoder at the front of the elevation shaft measures the angle of rotation in this position and outputs the pulse signal C to the motion controller. The readhead located below the magnetic scale outputs the pulse signal D to the motion controller. By comparing pulse signal A with pulse signal D, the error caused by the backlashes between the driving gear and the elevation gear can be measured. By comparing pulse signal C with pulse signal D, the error caused by the centerline deviation of the bearings at both ends of the elevation shaft can be measured.

2.2. Error Analysis of Encoders. The measurement terminals used in this study include the encoder that comes with the servo motor, the encoder connected to the end of the elevation shaft, and the magnetic encoder system. The precise installation of these measurement terminals is the basis for ensuring the accuracy of the measurement results. Therefore, it is necessary to analyze the encoder's own errors and reduce their interference with the measurement results.

The eccentricity error of the magnetic scale in the magnetic encoder system will seriously affect its accuracy. This eccentricity error is caused when the geometric center of the magnetic scale does not coincide with the actual center of rotation during installation, as shown in Figure 2.

The installation radius of the magnetic scale is R, O is the center of the magnetic scale, O' is the center of the magnetic scale after eccentricity, and the eccentricity is e. Assuming that the actual rotation angle and the theoretical rotation angle of the magnetic scale are β_1 and β, respectively, equations (1) and (2) can be obtained according to the geometric relationship in Figure 2.

$$\tan\beta_1 = \frac{R\sin\beta}{R\cos\beta - e}, \tag{1}$$

$$\tan\Delta\beta = \tan\left(\beta_1 - \beta\right) = \frac{e\sin\beta}{R - e\cos\beta}. \tag{2}$$

When $\Delta\beta$ is sufficiently small, $\tan\alpha \approx \alpha$. Since R is much larger than $e\cos\beta$, equation (2) is simplified to obtain the following equation:

$$\Delta\beta \approx \frac{e\sin\beta}{R}. \tag{3}$$

Based on the working principle of an encoder, we know that encoders continuously process the signal sampled by the front end through the microprocessor. However, the signal is not synchronized in time from the time it is sampled to the time it enters the microprocessor for position angle calculation. This dynamic angle error due to system delay is easy to ignore among many error factors. Assuming that the time delay from when the signal is sampled to when the microcontroller starts the corresponding solution is Δt, and the rotational angular velocity of the elevation shaft is ω, the dynamic delay error can be expressed by the following equation within the delay time Δt.

$$e_d = \Delta t \cdot \omega. \tag{4}$$

Figure 3 shows the relationship between the dynamic delay error and the rotational angular velocity for different delay times [21]. It can be seen that the dynamic delay error is proportional to the rotational angular velocity. In high-speed rotation, the error caused by the dynamic delay angle has a great impact on the accuracy of the encoder.

On the basis of the analysis of the encoder's own errors and the parameters of the experimental platform, the maximum value of the eccentricity error of the magnetic scale installation and the dynamic delay error of the encoder are calculated. In the experimental platform, the maximum speed of the elevation shaft is about 1°/s, and the installation radius of the magnetic scale is 71.5 mm. If the delay time is 0.6×10^{-3} s, then the encoder dynamic delay error can be calculated as 2.06″ according to equation (4) and Figure 3. If the eccentricity between the geometric center and the center of rotation of the magnetic scale is 10 μm, the maximum

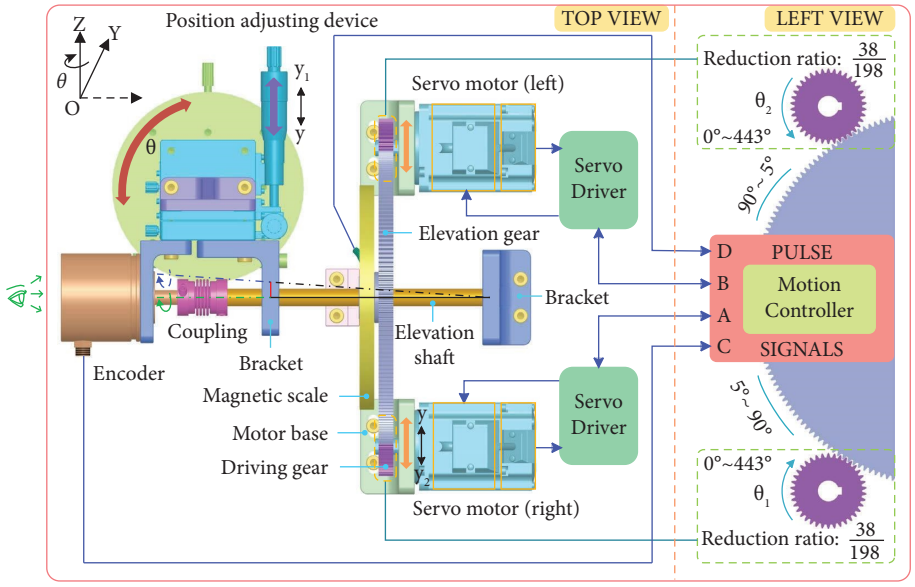

Figure 1: The measurement principle of the error of the elevation mechanism.

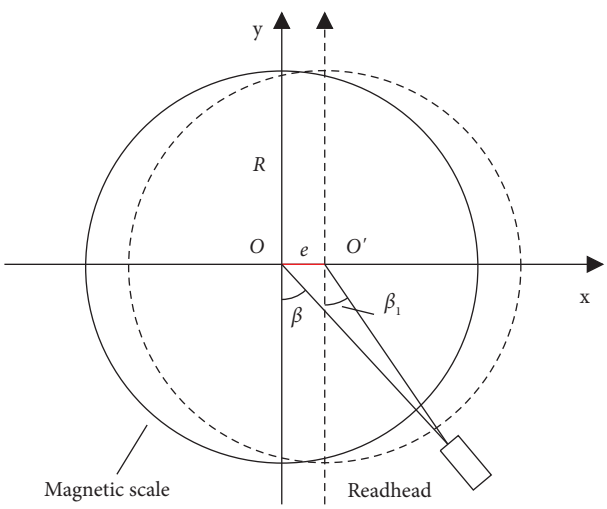

Figure 2: The installation eccentricity error of the magnetic encoder system.

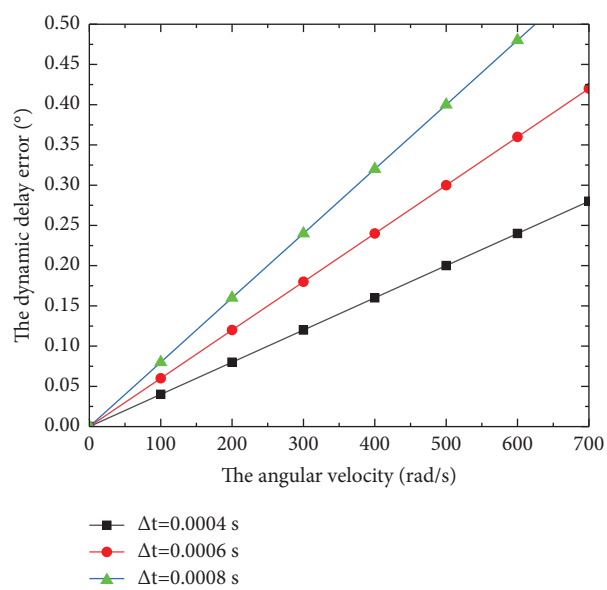

Figure 3: The relationship between the dynamic delay error and the rotational angular velocity.

value of the eccentricity error of the magnetic scale installation is 0.5″ according to equation (3). It can be seen that the errors caused by the encoder itself are on the order of angular seconds or even subangular seconds.

2.3. Building Experiment Platform. After analyzing the measurement method and the principle of antenna elevation mechanism error, it is also necessary to design the scaled-down experiment platform for error measurement according to its operating environment and actual working conditions. In actual antenna working conditions, the elevation gear is driven by the dual-motor, and the error caused by the backlash is generally removed by both mechanical and electrical backlash elimination methods. After long-term operation and wear of the elevation gear, the error caused by the backlash cannot be eliminated by electrical means, so it is necessary to measure the law of change of the mechanical backlash error. Furthermore, the measurement of the angle of elevation during antenna operation can only be performed by the encoder at the end of the elevation shaft, and the measured value of the encoder has been mixed with various error factors after passing through multiple drive chains. Therefore, it is necessary to measure and compare the errors of each transmission chain of the elevation shaft and to determine their law of change by multiencoder information sources.

Based on the analysis presented above, this study builds the scaled-down experimental platform for measuring antenna elevation mechanism error, as shown in Figure 4.

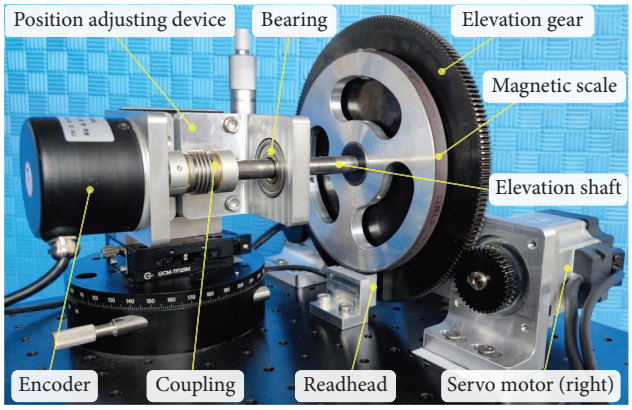

Figure 4: The measurement experiment platform of the error of the elevation mechanism.

The operating principle of the experimental platform in Figure 4 is the same as the error measurement principle described in Subsection 2.1.

3. Experiments and Results

According to the analysis of the antenna elevation mechanism error in the previous section, the real-time positions of different parts of the elevation mechanism are measured and recorded by using a multiencoder to collect pulse signals from multiple positions simultaneously. Measurements and recordings are divided into four cases: elevation action driven by a single motor, elevation action driven by two motors, elevation action under different centerline deviations of the bearings, and elevation action under different backlashes.

3.1. The Elevation Action Driven by the Single Motor. When the elevation gear is driven by a single motor, the elevation shaft rotates from 5° to 90° at a speed of 1°/s. Referring to Figure 1, it can be seen that signal D-signal A represents the backlash error between the elevation gear and the driving gear, and signal D-signal C represents the error caused by the centerline deviation of the bearings at both ends of the elevation shaft. As can be seen in Figure 5 that when the elevation shaft rotates from 5° to 90°, that is, the antenna is pitched up, the transmission error caused by the backlash error and the centerline deviation of the bearings continues to increase, and the backlash error increases faster. When the elevation shaft rotates to 90°, the backlash error reaches 0.4°.

In order to further observe the law of change of the two errors in the complete elevation action of the antenna, we then rotated the elevation shaft from 5° to 90° and then from 90° to 5° at a speed of 1°/s. The rotation of the elevation shaft is suspended at 90° for 1 second to eliminate interference from rotational inertia. The error results are shown in Figure 6. It can be seen from the figure that the transmission error caused by the backlash error and the centerline deviation of the bearings decreases with the pitched down action of the antenna. Both errors are close to zero when the elevation shaft rotates back to 5°.

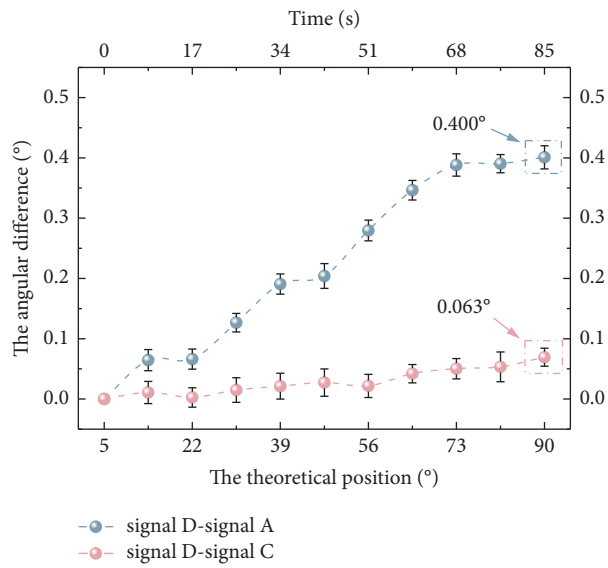

Figure 5: The angle difference of the single-motor drive (5°~90°).

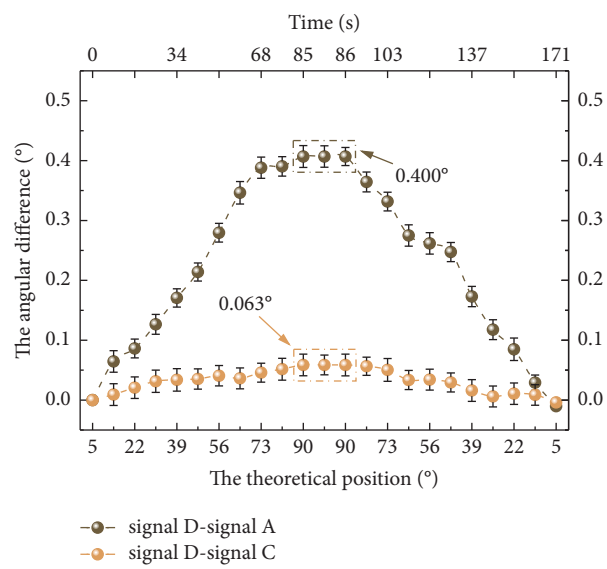

Figure 6: The angle difference of the single-motor drive (5°~90°~5°).

Combining Figures 5 and 6, it can be seen that when the elevation shaft is driven by a single motor, the transmission error caused by the backlash error and the centerline deviation of the bearings will gradually increase when the antenna is elevated during a complete elevation cycle. The maximum is reached when the antenna is rotated to 90°, which are 0.4° and 0.063°, respectively. When the antenna is pitched down, the two kinds of error will gradually decrease; the errors approach zero when the antenna is rotated to 5°. This error law of change is a nonlinear elastic error.

3.2. The Elevation Action Driven by the Dual-Motor. To compare the error law of change when driven by the single motor and the dual motor, as well as the effect of the dual motor on the elimination of mechanical backlash, a motor is

installed on each side of the elevation gear, respectively, as shown in Figure 7. The right motor drives the elevation gear from 5° to 90° at a speed of 1°/s, and the left motor drives the elevation gear from 90° to 5° at a speed of 1°/s. That is, the right motor drives the antenna pitched up, and the left motor drives the antenna pitched down. This process can ensure that the elevation gear always engages with the driving gear.

When the dual-motor drives the elevation gear, the error results are shown in Figure 8. It can be seen from the figure that the transmission error caused by the backlash error and the centerline deviation of the bearings gradually increases as the antenna's elevation increases and reaches the maximum value of 0.128° and 0.062°, respectively, when the antenna rotates to 90°. The two kinds of error gradually decrease as the elevation gear rotates back. The change trend and law of the two types of error are similar to those of the elevation gear driven by a single motor, and they are both nonlinear elastic errors.

Comparing Figures 6 and 8, it can be seen that when the antenna performs the elevation action, the error caused by the backlash is significantly reduced by adopting the dual-motor driving method. It shows that the dual-motor driving method has a good mechanical backlash elimination effect. However, it can also be seen that the dual-motor driving method does not have a significant effect on the error caused by the centerline deviation of the bearings.

3.3. The Elevation Action under Different Centerline Deviations of the Bearings. When the antenna is installed, or after a period of operation, the centerline of the bearings at both ends of the elevation shaft will deviate. Therefore, it is necessary to measure the transmission error caused by the centerline deviation of the bearings and analyze the error law of the change at different degrees. The centerline deviation of the bearings can occur randomly in the radial direction of the bearings. In this study, the centerline deviation of the bearings along the Y axis is taken as an example. Before installing the elevation gear, we used a dial indicator to measure along the axis of the elevation shaft. At the same time, we continuously adjust the Z axis of the position adjusting device so that the heights of both ends of the elevation shaft in the direction of the Z axis are consistent, as shown in Figure 9.

After adjusting the heights of both ends of the elevation shaft along the direction of the Z axis, it is also necessary to adjust its position along the direction of the Y axis. Again, we use a dial indicator to measure along the axial direction of the elevation shaft and continue to adjust the Y axis of the position adjusting device so that the position of both ends of the elevation shaft along the direction of the Y axis is consistent, as shown in Figure 10. After adjusting the positions of both ends of the elevation shaft along the directions of the Z axis and the Y axis, we use this as an initial reference. By changing the y_1 of the position adjusting device along the direction of the Y axis and the rotation angle θ around the center, the centerline deviation of the bearings increases by 0.5 mm. The values of y_1 and θ are given in Table 1.

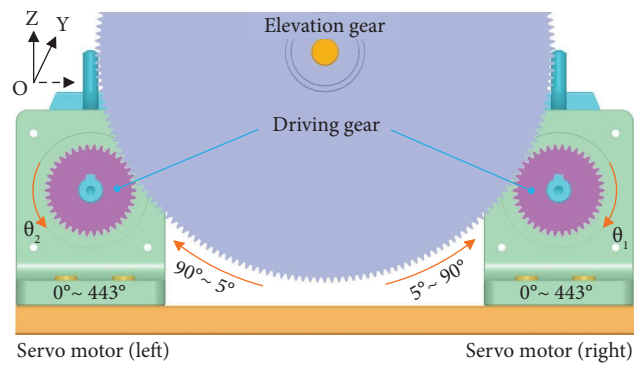

Figure 7: Schematic of dual-motor drive.

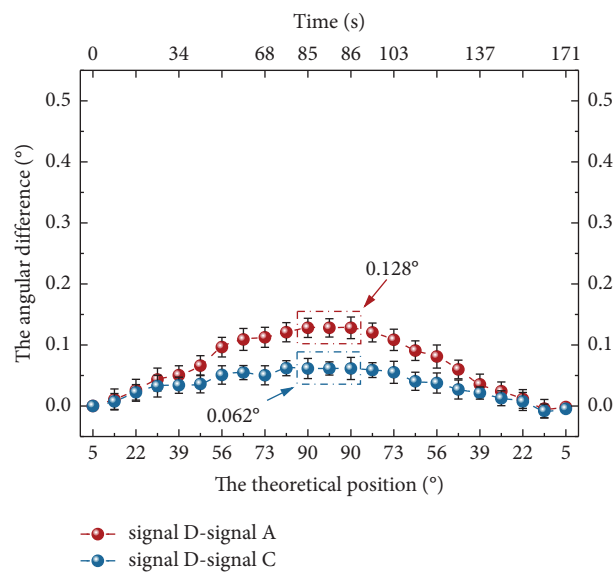

Figure 8: The angle difference of dual-motor drive (5°~90° driven by the right motor, 90°~5° driven by the left motor).

Referring to Figure 10, since the right end of the elevation shaft is fixed, when the value of y_1 increases, the elevation shaft will be slightly deformed due to the bending moment. In this case, it is necessary to fine-tune the rotation angle θ around the center of the position adjustment device to eliminate the impact of deformation at both ends of the elevation shaft as much as possible. According to the geometric relationship in Figure 10, it can be obtained as follows:

$$\begin{aligned}\theta &= \arctan \angle P_2P_1P_3 \\ &= \arctan \frac{y_1}{b}.\end{aligned} \tag{5}$$

In equation (5), b is the center distance of the bearings at both ends of the elevation shaft.

In the experimental platform, the bearing center distance at both ends of the elevation shaft is 150 mm, so the relationship between the rotation angle θ of the center of the position adjusting device and y_1 is shown in Table 1:

The right motor was controlled to drive the elevation shaft rotated from 5° to 90° and then rotated back to 5° at

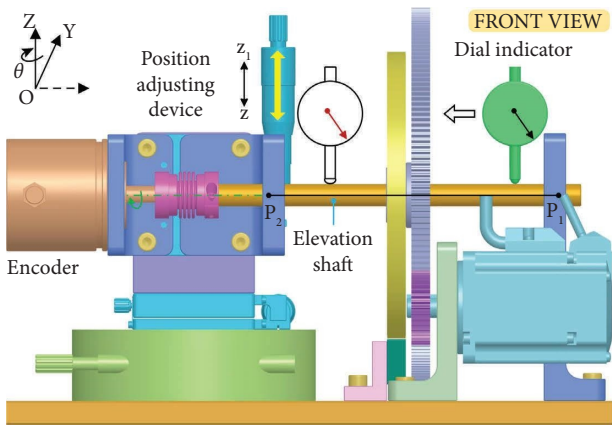

Figure 9: The elevation shaft is adjusted in the direction of the Z axis.

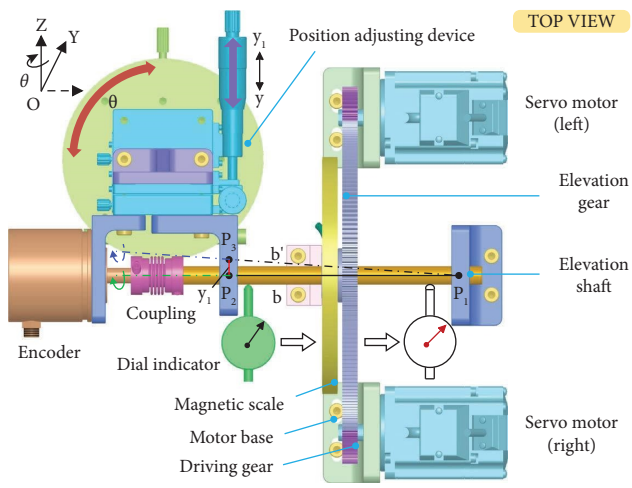

Figure 10: The elevation shaft is adjusted in the direction of the Y axis.

Table 1: The relationship between y_1 and θ.

y_1 (mm)	0	0.5	1.0	1.5
θ (°)	0	0.19	0.38	0.57

a speed of 1°/s. Transmission error was measured under the four centerline deviations of the bearings of $y_1 = 0$ mm, $y_1 = 0.5$ mm, $y_1 = 1.0$ mm, and $y_1 = 1.5$ mm, respectively, and the error results are shown in Figure 11.

It can be seen in Figure 11 that different centerline deviations of the bearings will cause different transmission errors, and the law of change of transmission errors still belongs to nonlinear elastic errors. Furthermore, by comparing Figures 11(a)–11(d), it can be seen that with increasing y_1, the maximum value of transmission error caused by centerline deviation of the bearings at both ends of the elevation shaft also increases at a constant rate. In Figure 11(d), when the centerline deviation of the bearings at both ends of the elevation shaft is 1.5 mm, the maximum transmission error caused by it reaches 0.257° in one complete elevation cycle of the antenna.

3.4. The Elevation Action under Different Backlashes. In Subsection 3.1, when analyzing the elevation action driven by the single-motor, it is found that there is a certain law in the change of the backlash error when the driving gear meshes with the elevation gear. The change of this error is further analyzed under different backlashes.

The variation of backlash in the gear transmission structure is related to the negative tolerance of the tooth thickness and the center distance, and their geometric relationship is shown in Figure 12. Referring to Figure 12, it can be seen that the size of the tooth clearance is proportional to the negative tolerance of the tooth thickness and the center distance of the gear, respectively. By adjusting the displacement y_2 of the motor base along the direction of the Y axis, the center distance between the elevation gear and the driving gear can be changed, and then the backlash can be adjusted. When the driving gear meshes with the elevation gear, the minimum backlash between them can be calculated according to equation [22] as follows:

$$J_{\min} = \frac{2(0.06 + 0.0005a + 0.03mn)}{3}. \tag{6}$$

In equation (6), $J_{\min}$ is the minimum backlash, a is the center distance, m and n are the modulus of the two gears, respectively.

In the experimental platform, the elevation gear and the driving gear parameters are shown in Table 2. It can be calculated that the center distance between the two gears $a = 118$ mm and the minimum backlash $J_{\min} \approx 0.1$ mm. The position of y_2 at this time is marked as 0, and the backlash of the two gears is adjusted based on this position.

In terms of geometric relationship, the minimum backlash $J_{\min}$ between the elevation gear and the driving gear is not directly equal to the displacement y_2 of the driving gear along the direction of the Y axis. As shown in Figure 13, there is the following geometric relationship between $J_{\min}$ and y_2:

$$\frac{a}{d/2} = \frac{y_2}{J_{\min}}. \tag{7}$$

In equation (7), d is the reference diameter of the elevation gear.

According to the geometric relationship between $J_{\min}$ and y_2 in Figure 13 and the parameters of the two gears in Table 2, the corresponding relationship between the displacement y_2 of the driving gear along the direction of the Y axis and the minimum backlash $J_{\min}$ between the two gears can be obtained, as shown in Table 3.

Controlling the motor on the right to drive the elevation shaft from 5° to 90° and then rotating back from 90° to 5° at a speed of 1°/s, the errors of four displacements of $y_2 = 0$ mm, $y_2 = 0.5$ mm, $y_2 = 1.0$ mm, and $y_2 = 1.5$ mm were measured, respectively, and the results are shown in Figure 14.

As can be seen in Figure 14, the change in the minimum backlash $J_{\min}$ causes the backlash error to change. By comparing Figures 14(a)–14(d), it can be seen that the backlash error when the driving gear meshes with the elevation gear increases continuously with the increase in $J_{\min}$.

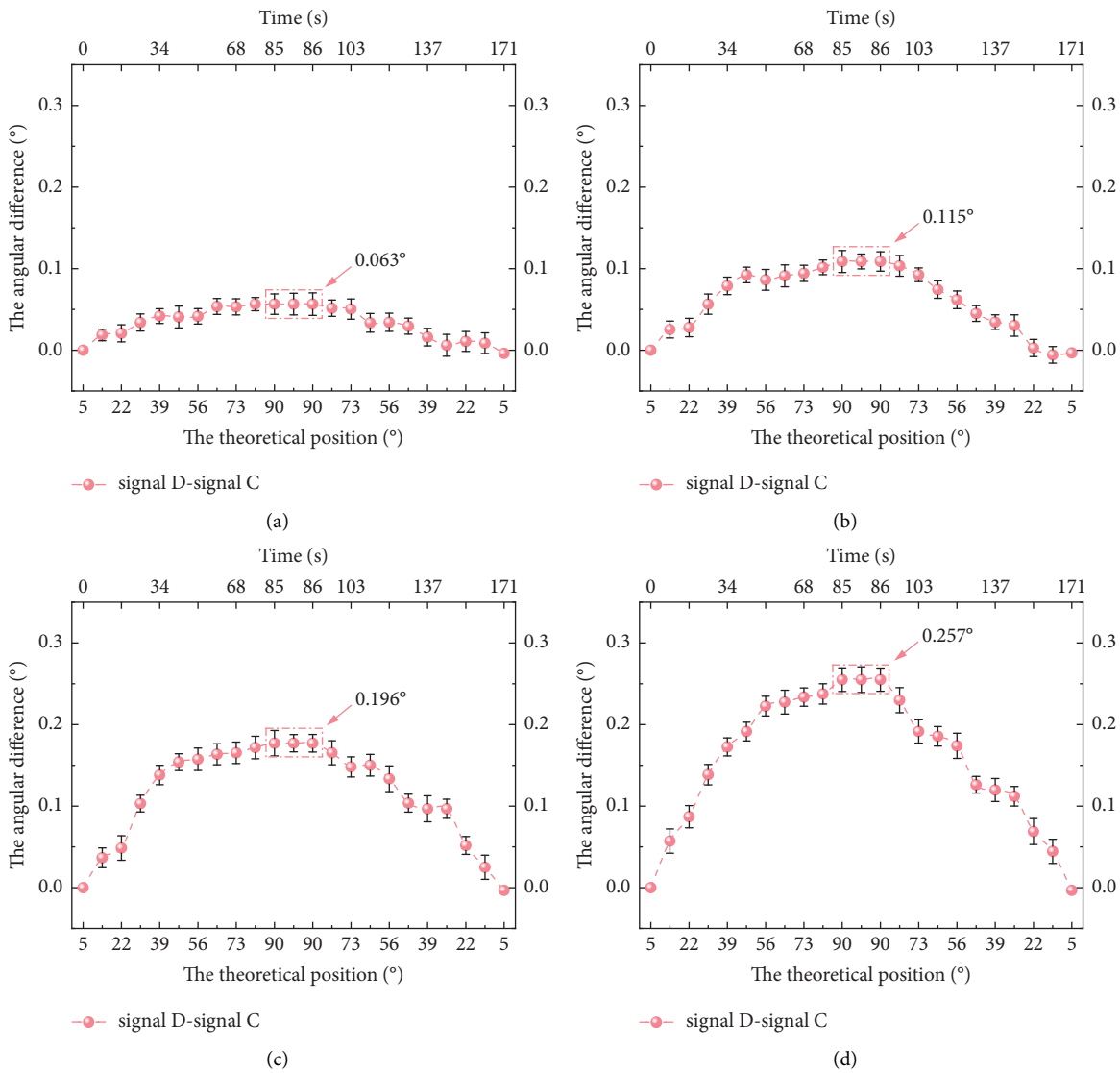

Figure 11: The angle difference of different centerline deviations of bearings. (a) $y_1 = 0$ mm. (b) $y_1 = 0.5$ mm. (c) $y_1 = 1.0$ mm. (d) $y_1 = 1.5$ mm.

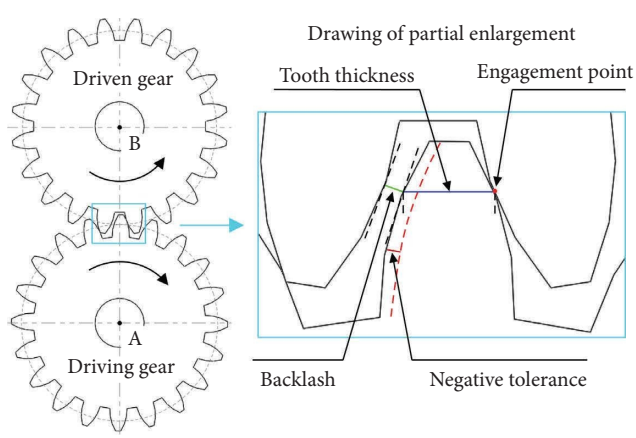

Figure 12: The geometric relationship of backlash in gear transmission structure.

Table 2: The parameters of the two gears.

	Number of teeth	Modulus	Reference diameter (mm)
Elevation gear	198	1	198
Driving gear	38	1	198

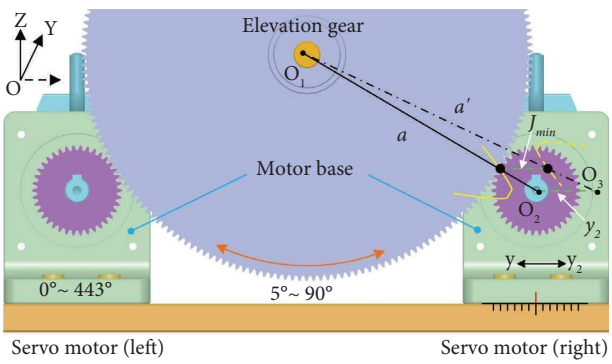

Figure 13: The geometric relationship between $J_{\min}$ and y_2.

Table 3: The corresponding relationship between y_2 and $J_{\min}$.

y_2 (mm)	0	0.5	1.0	1.5
$J_{\min}$ (mm)	0.1	0.42	0.84	1.26

As shown in Figure 14(d), when y_2 is 1.5 mm, that is, $J_{\min}$ is 1.26 mm, the backlash error between the elevation gear and the driving gear reaches the maximum value of 0.969° in a complete antenna elevation cycle.

4. Comparison and Analysis

In the previous section, elevation action experiments were carried out for the antenna elevation shaft with the single-motor drive and the dual-motor drive. Under the two different drive modes, the backlash error and the transmission error caused by the centerline deviation of the bearings have different effects. Additionally, the elevation action under different centerline deviations of the bearings and different backlashes will also cause different errors. This section further compares and analyses these errors.

4.1. The Error Caused by the Driving Modes. Figure 15 shows the standard deviation, mean value, and maximum value of the errors caused by the backlash when the elevation shaft is driven by the single-motor and the dual-motor, respectively. In this plot, the standard deviation reflects the dispersion of the error caused by the backlash over a complete elevation cycle of the antenna.

As can be seen in Figure 15, when the elevation shaft driving mode changes from the single-motor drive to the dual-motor drive, the mean value of the error caused by the backlash is reduced from 0.21° to 0.06°, decreasing by 71.4%. This indicates that the drive of the dual-motor has a greater effect in eliminating the error caused by the backlash compared to the single-motor drive. Moreover, in terms of standard deviation, the error caused by backlash is relatively less dispersed when the elevation shaft is driven by the dual motor.

The standard deviation, mean value, and maximum value of the transmission error caused by the centerline deviation of the bearings are shown in Figure 16.

It can be seen in Figure 16 that the mean value of the transmission error caused by the centerline deviation of the bearings is 0.032° for both drive modes, and the standard deviation and the maximum value are also approximately equal.

4.2. The Error Caused by the Centerline Deviation of the Bearings. The standard deviation, mean value, and maximum value of errors caused by the centerline of bearings at the four types of deviation values are shown in Figure 17.

It can be seen from Figure 17 that the standard deviation, mean value, and maximum value of the transmission error caused by the centerline deviation of the bearings all increase with the increase of the deviation value. When the deviation value is 0, the mean value of the transmission error caused by the centerline deviation of the bearings is 0.03° in one complete elevation cycle of the antenna. This average error may be caused by the slight deformation of the elevation shaft during the antenna elevation process. When the deviation value increases from 0 to 1.5 mm, the mean value of the transmission error caused by the deviation value increases from 0.03° to 0.15°, which is an increase of about 5 times.

4.3. The Error Caused by the Backlash. The standard deviation, mean value, and maximum value of errors caused by the four types of backlash when the driving gear meshes with the elevation gear are shown in Figure 18.

It can be seen in Figure 18 that the standard deviation, mean value, and maximum value of the error caused by the backlash all increase as it increases. When the minimum backlash between the elevation gear and the driving gear is 0.1 mm, the mean value of the error caused by this backlash is 0.22°. When the minimum backlash increases from 0.1 mm to 1.26 mm, the average error caused by the backlash increases by 1.9 times. This also shows that the antenna error during the elevation process is greatly affected by the change in backlash.

The error variation law of the elevation mechanism caused by multiple error factors measured in the experimental platform is important for improving the pointing accuracy of the radio telescope directly or indirectly.

During the pointing of the radio telescope, the motor adjusts the elevation angle by a signal from the control room, while the actual elevation angle is fed back to the control room by an encoder at the end of the elevation shaft. According to the experimental results, different driving modes of the elevation mechanism affect the actual elevation angle of the encoder feedback. Therefore, at the beginning of the design of the radio telescope, the elevation shaft needs to be driven by multiple motors to reduce the deviation

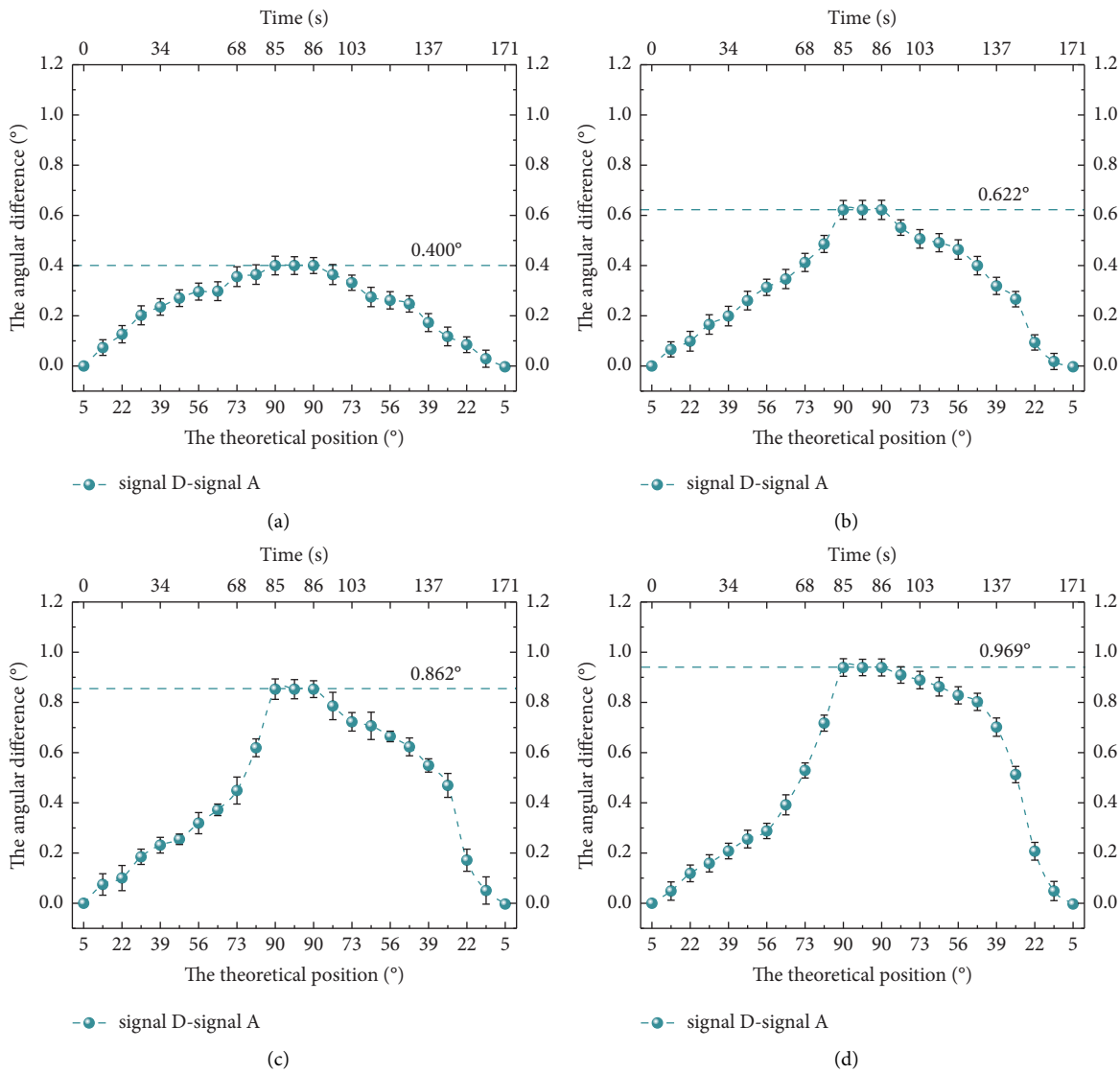

Figure 14: The angle difference of different backlashes. (a) $y_2 = 0$ mm, $J_{min} = 0.1$ mm; (b) $y_2 = 0.5$ mm, $J_{min} = 0.42$ mm; (c) $y_2 = 1.0$ mm, $J_{min} = 0.84$ mm; (d) $y_2 = 1.5$ mm, $J_{min} = 1.26$ mm.

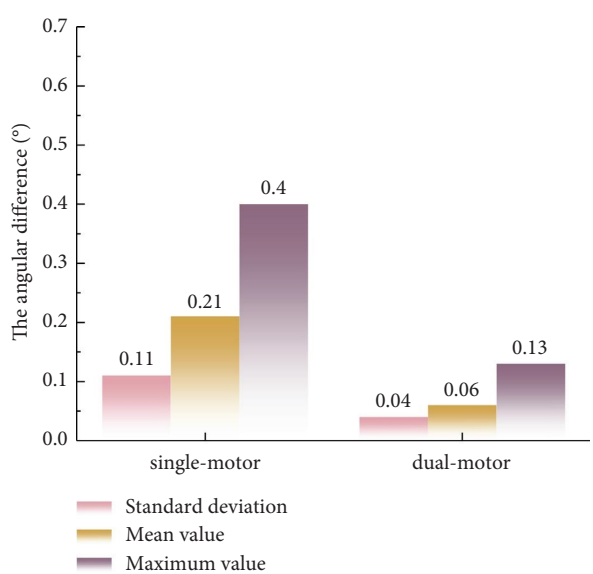

Figure 15: The error caused by the backlash.

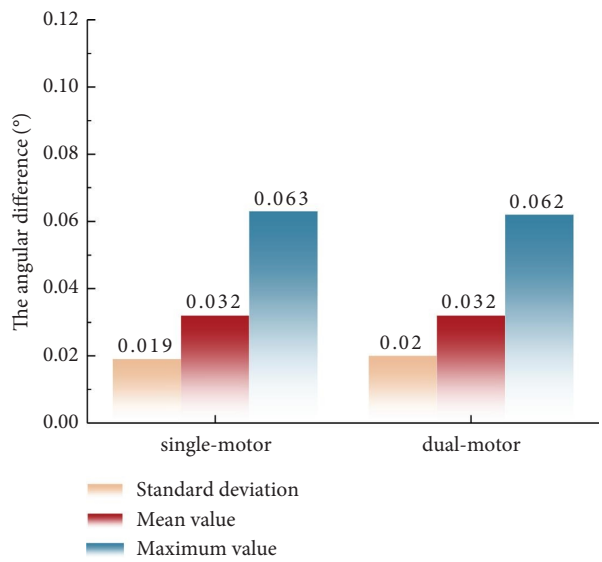

Figure 16: The error caused by the centerline deviation of the bearings.

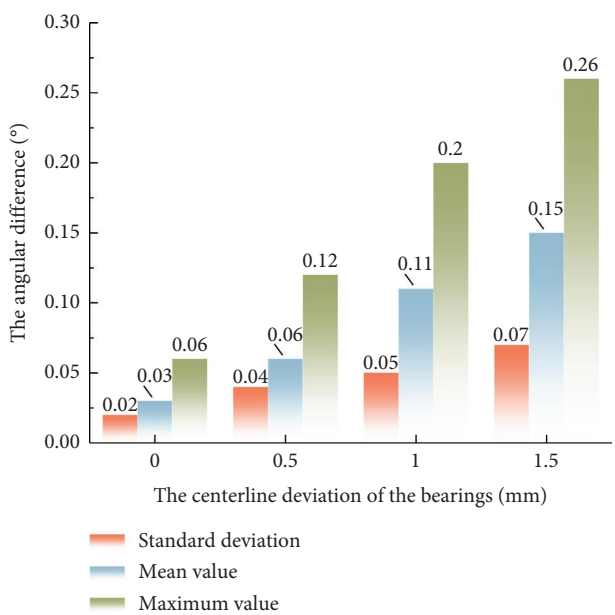

Figure 17: Comparison of errors under the four types of deviation values.

between the actuation angle and the feedback angle of the elevation mechanism. In addition, a more efficient way is to compensate the actuation angle of the elevation mechanism in the control signal according to the error variation law measured in the experiment.

The centerline deviation of the bearings at both ends of the elevation shaft is generated during the installation or operation of the radio telescope. Although the direction of the centerline deviation is random, the components of this deviation in the x, y, and z directions can be measured and calculated at the radio telescope. According to the relationship between the centerline deviation of the bearings and transmission error in the experimental results, the error

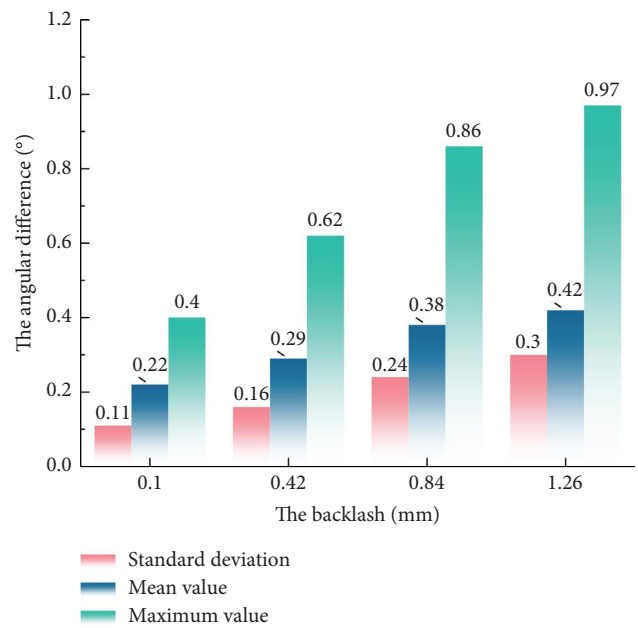

Figure 18: The error comparison under the four types of backlash.

caused by the centerline deviation of the bearings can be corrected in the existing error correction model.

Wear between the elevation gear and the driving gear during the long-term operation of the radio telescope can reduce the fatigue life of the gear material. It also leads to the continuous expansion of the backlash, which affects the pointing accuracy of the radio telescope. According to the variation law of backlash and error in the experimental results, the reasonable arrangement and dynamic adjustment of the observation plan of the radio telescope can help reduce the wear of the transmission gear, prolong the fatigue life of the gear material, and reduce the error of the elevation mechanism.

5. Conclusions

The pointing errors of large aperture radio telescopes directly affect their observation results. Measurement and analysis of the error of its various parts are an important means of improving pointing errors. Aiming at the error factors caused by the elevation shaft of the radio telescope, this study measured and analyzed the law of change of the elevation shaft rotation error under different driving modes, different centerline deviations of the bearings, and different backlashes.

When the driving mode of the elevation shaft was changed from single-motor drive to dual-motor drive, the maximum value of the error caused by the backlash between the elevation gear and the driving gear was reduced from 0.4° to 0.13°, and the mean value was reduced from 0.21° to 0.06°. This shows that the driving mode of the dual-motor can eliminate about 70% of the mechanism error caused by the backlash. However, the change in driving mode will hardly affect the error caused by the centerline deviation of the bearings at both ends of the elevation shaft.

When the centerline of the bearings at both ends of the elevation shaft has different deviation values, it will affect the transmission error of the elevation shaft. Experiments show that when the deviation value increases from 0 to 1.5 mm, the mean value of the transmission error caused by the deviation value increases from 0.03° to 0.15°, which is an increase of about 5 times.

When the minimum backlash between the elevation gear and the driving gear increased from 0.1 mm to 1.26 mm, the mean value of the error caused by this backlash increased by a factor of 1.9.

From the results of measurement and analysis, factors such as the driving mode of the elevation shaft, the backlash, and the centerline deviation of the bearings will greatly affect the rotation error of the elevation shaft. Therefore, in the design of radio telescopes, the way multiple motors drive the elevation shaft should be considered. The measurement results can also be applied to the control program and error correction model to obtain a more accurate elevation angle. It is also possible to adjust the observation time and observation plan dynamically in future observations, so as to ensure the long-term stable pointing accuracy of the radio telescope. The research results have important reference values for the correction of the pointing errors of the existing Nan Shan 26 m radio telescope and the Qi Tai 110 m radio telescope to be built.

Data Availability

The data that support the findings of this study are available from the corresponding author (xuqian@xao.ac.cn) upon reasonable request.

Conflicts of Interest

The authors declare that they have no conflicts of interest.

Acknowledgments

This work was supported by the National Natural Science Foundation of China (grant no. 12273102), the Natural Science Foundation of Xinjiang Autonomous (grant no. 2022D01E85), the Youth Innovation Promotion Association, CAS (grant no. Y202019), the National Key Research and Development Program of China (grant no. 2021YFC2203601), the Operation, Maintenance and Upgrading Fund for Astronomical Telescopes and Facility Instruments, budgeted from the Ministry of Finance of China (MOF) and administrated by the Chinese Academy of Sciences (CAS), and the Scientific Instrument Developing Project of the Chinese Academy of Sciences (grant no. PTYQ2022YZZD01).

References

[1] N. Wang, "Xinjiang Qitai 110 m radio telescope," *Scientia Sinica*, vol. 44, no. 8, 2014.

[2] B. Du, Y. Zheng, and Y. Zhang, "Progress in SHAO 65m radio telescope antenna," in *Proceedings of the International Symposium on Antennas & Propagation*, Nanjing, China, October 2013.

[3] R. Wielebinski, N. Junkes, and B. H. Grahl, "The effelsberg 100-m radio telescope: construction and forty years of radio astronomy," *Journal of Astronomical History and Heritage*, vol. 14, no. 01, pp. 3–21, 2011.

[4] R. M. Prestage, K. T. Constantikes, T. R. Hunter et al., "The Green Bank Telescope," *Proceedings of the IEEE*, vol. 97, no. 8, pp. 1382–1390, 2009.

[5] E. White, F. D. Ghigo, R. M. Prestage et al., "Green Bank Telescope: overview and analysis of metrology systems and pointing performance," *Astronomy & Astrophysics*, vol. 659, 2022.

[6] D. Q. Kong, S. G. Wang, J. Q. Wang, M. Wang, and H. B. Zhang, "A new calibration model for pointing a radio telescope that considers nonlinear errors in the azimuth axis," *Research in Astronomy and Astrophysics*, vol. 14, no. 6, pp. 733–740, 2014.

[7] L. Huang, W. Ma, and J. Huang, "Modeling and calibration of pointing errors with alt-az telescope," *New Astronomy*, vol. 47, pp. 105–110, 2016.

[8] W. Chen, Z. Wang, and X. Zhou, "An improved radio pointing model for SHARC II of the caltech submillimeter observatory telescope," *Publications of the Astronomical Society of the Pacific*, vol. 134, no. 1040, Article ID 105002, 2022.

[9] W. Gawronski, F. Baher, and E. Gama, "Track level compensation look-up table improves antenna pointing precision," in *Proceedings of the Optomechanical Technologies for Astronomy. SPIE*, Orlando, FL, USA, July 2006.

[10] E. Maneri and W. Gawronski, "A method and a graphical user interface for the creation of an azimuth-track-level look-up table," *Interplanetary Network Progress Report*, vol. 143, pp. 1–17, 2000.

[11] F. Buffa, A. Causin, A. Cazzani et al., "The Sardinia Radio Telescope: a comparison between close-range photogrammetry and finite element models," *Mathematics and Mechanics of Solids*, vol. 22, no. 5, pp. 1005–1026, 2017.

[12] B. Nikolic, R. M. Prestage, D. S. Balser, C. J. Chandler, and R. E. Hills, "Out-of-focus holography at the Green Bank Telescope," *Astronomy & Astrophysics*, vol. 465, no. 2, pp. 685–693, 2007.

[13] I. Hashimoto, M. Chiba, N. Okada et al., "Wind- and operation-induced vibration measurements of the main reflector of the Nobeyama 45 m radio telescope," *Journal of Vibration Engineering & Technologies*, vol. 8, no. 6, pp. 909–923, 2020.

[14] M. K. Cho, L. M. Stepp, and G. Z. Angeli, "Wind loading of large telescopes," in *Proceedings of the Large Ground-Based Telescopes. SPIE*, Waikoloa, HI, USA, February 2003.

[15] N. Ukita, "Thermal effects on the pointing of the Nobeyama 45-m telescope," *Publications of the National Astronomical Observatory of Japan*, vol. 5, no. 4, pp. 139–147, 1999.

[16] F. Fan, X. Jin, and S. Shen, "Effect of non-uniform solar temperature field on cable-net structure of reflector of large radio telescope-FAST," *Advances in Structural Engineering*, vol. 12, no. 4, pp. 503–512, 2009.

[17] D. Q. Kong, Z. Y. Jiang, and H. B. Zhang, "Effects of sunshine temperature on axis angle measurement errors of large radio telescopes and the correction method (in Chinese)," *Sci Sin Tech*, vol. 49, pp. 1331–1342, 2019.

[18] Y. Zheng, G. Liu, and C. Jin, "Structure design and performance realization of radio telescope antennas," *Radio Engineering*, vol. 48, no. 11, pp. 913–919, 2018.

[19] A. Fernandez-del-Rincon, P. Garcia, A. Diez-Ibarbia, A. de-Juan, M. Iglesias, and F. Viadero, "Enhanced model of gear transmission dynamics for condition monitoring applications: effects of torque, friction and bearing clearance," *Mechanical Systems and Signal Processing*, vol. 85, pp. 445–467, 2017.

[20] Z. Liu, Z. Liu, J. Zhao, and G. Zhang, "Study on interactions between tooth backlash and journal bearing clearance nonlinearity in spur gear pair system," *Mechanism and Machine Theory*, vol. 107, pp. 229–245, 2017.

[21] H. Shen and M. Wang, "High-precision magnetic encoder module design based on real-time error compensation algorithm," *Journal of Physics: Conference Series*, vol. 1345, no. 4, Article ID 042082, 2019.

[22] D. T. Qin and L. Y. Xie, *Modern Mechanical Design Manual*, Chemical Industry Press, Beijing, China, 2011.